MATHEMATICAL MODELING OF HIGH-FREQUENCY MAGAMP SWITCH B-H CHARACTERISTIC

Anna Yaskiv[1], Keyue Smedley[2], Alexander Abramovitz[3], Volodymyr Yaskiv[4], Natalia Kasatkina[5]

[1]West Ukrainian National University, 11 Lvivska str., Ternopil, Ukraine, 46009; annyaskiv@gmail.com
[2]University of California, Irvine, Irvine, CA 92697-2625, USA, smedley@uci.edu
[3]Holon Institute of Technology, 52 Golomb str., Holon 5810201, Israel; alabr@hotmail.com
[4]Ternopil Ivan Puluj National Technical University, 56 Ruska str., Ternopil, Ukraine, 46001; yaskiv@yahoo.com
[5]National University of Food Technology, 68 Volodymyrska str., Kyiv, Ukraine, 03001; nkasatkina@ukr.net

Abstract: The current paper features a problem of high-frequency MagAmp switch modeling for computer aided design programmes to enable MagAmp power converters design automation. A new mathematical model of MagAmp switch B-H characteristic is presented. An algorithm of its computer integration is described. Dependence of B-H characteristic on switching frequency is investigated for two configurations of MagAmp switches with cores of amorphous Co-based alloy with rectangular hysteresis loop. The simulation results are obtained, and maximum modeling error is calculated.

Keywords*: high-frequency MagAmp switch, B-H characteristic, magnetic hysteresis, mathematical model, computer simulation.*

1. Introduction

High-frequency MagAmp switches are used in pulse power converters when it is necessary to provide high reliability, efficiency, high level of dynamic characteristics [1,2]. They do not require complicated control circuits, PWM controllers, input rectifiers, leading to simpler power supplies' topologies, smaller number of components, mass and dimensions, and, consequently, reduced price of the device along with its increased reliability and efficiency. Such power converters are widely used in aviation, biomedical, space, lighting engineering, communications and IT, transport systems, etc. [3-6].

MagAmp switch consists of a core made of soft magnetic material with relatively square B-H characteristic, winding around it, and is supplemented with a diode to block applied voltage when necessary [7]. If MagAmp switch configuration turns out to be wrong for the required power supply specification, it has to be soldered out and formed again as a component with adjusted number of winds around the core, leading to increased power converter design time complexity. The automation of power supplies design is achieved with computer aided design (CAD) programmes for electric circuits. However, such computer simulation is based on the discrete parameters of electric circuits such as currents and voltages, and is not suitable for modeling of magnetic fields and nonlinear magnetic components. That is why there is a problem of creation of MagAmp switch model suitable for its integration into a library of components of CAD programmes for electric circuits.

Nowadays there are CAD programmes for modeling solely magnetic fields [8-10]. There are integrations of Jiles-Atherton [11] and John Chan [12] models of magnetic hysteresis into pSim and LTspice environments respectfully, but they are suitable only for modeling MagAmp linear operation mode [13]. Preisach model of magnetic hysteresis [14] and artificial neural networks [15,16] feature high computational complexity and require integration into CAD programmes for electric circuits. The integration of analytical hysteresis model by A. Nicolaide into LabWiev software [17,18] is developed only for magnetic fields investigation and cannot be used for electric circuits design automation. MagAmp switch equivalent circuits have been developed [19] however, their parameters need to be calculated for each specific topology.

2. Proposed mathematical model of MagAmp switch B-H characteristic

Since MagAmp switching properties are defined by its B-H characteristic, it's crucial to develop its mathematical model that will be possible to integrate into CAD programmes. The hysteresis loop was split into 4 parts corresponding to different stages of MagAmp switching cycle (fig.1). It was decided to represent the steep parts with fragments of a sinusoidal function, since each CAD programme for electric circuits has a model of digital generator of sine waveforms in their components library [20]. However, digital generators of sinusoidal waveforms are not capable of recursive signal generation. It means, that they cannot be used to model the downward branch of B-H characteristic.

A microcontroller model can be programmed in the required way, also having an advantage of already inbuilt analogue-to-digital and digital-to analogue converters [20].

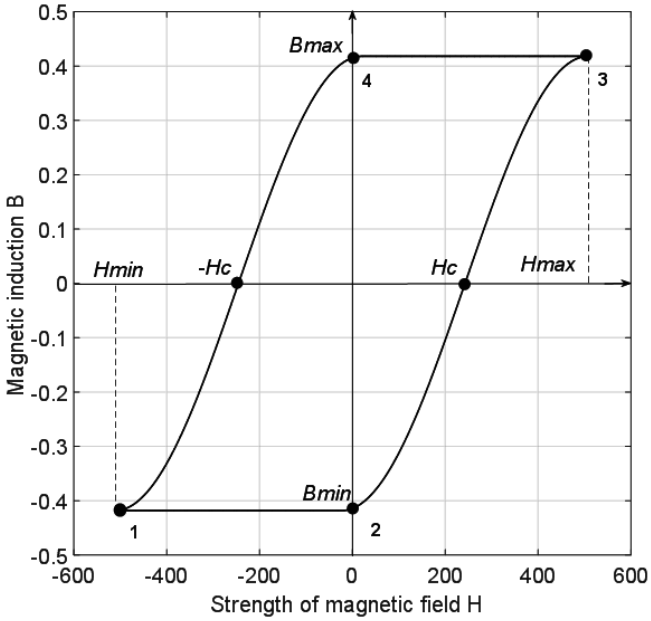

Fig. 1. Schematic diagram of MagAmp switch B-H characteristic, and the points that are crucial for its modeling

The curves that represent MagAmp core magnetization (parts 1-2, 2-3) and demagnetization (parts 3-4, 4-1) process can be mathematically described in the following way:

$$1-2:\begin{cases} g_n = g_{n-1}, \\ g_n = B_{\min}; \end{cases} \quad H_n = \overline{H_{\min}, H_{\min} + 2H_c}, B_n = B_{\min}, \tag{1}$$

$$2-3: g_n > g_{n-1}; \quad H_n = \overline{H_{\min} + 2H_c, H_{\max}}, B_n = k\sin(2\pi fnT_d + \varphi_1), \tag{2}$$

$$3-4:\begin{cases} g_n = g_{n-1}, \\ g_n = B_{\max}; \end{cases} \quad H_n = \overline{H_{\max}, H_{\max} - 2H_c}, B_n = B_{\max}, \tag{3}$$

$$4-1: g_n < g_{n-1}; \quad H_n = \overline{H_{\max} - 2H_c, H_{\min}}, B_n = k\sin(2\pi fnT_d + \varphi_2), \tag{4}$$

where g is a generated digital code that corresponds to a point on B-H characteristic. $n = \overline{1, N}$ — index of digital codes of electromagnetic variables, the other denotations are digital codes of corresponding constants. H_{min}, H_{max} are minimum and maximum values of strength of magnetic field respectfully. H_c is a coercive force. B_{min}, B_{max} are minimum and maximum values of magnetic induction respectfully. k is the amplitude of the waveform, for the full hysteresis loop $k=B_{max}$. For more simplicity, the current model suggests that saturation magnetic induction $B_s = B_{max}$, while in real physical systems B_{max} usually is magnetic induction value at $H=5H_c$ [20].

(1-4) constitute the mathematical model of MagAmp B-H characteristic. Saturation magnetic inductance B_s and coercive force H_c are its input parameters. They are the main magnetic characteristics of MagAmp cores and can be found in any MagAmp datasheet.

3. B-H characteristic mathematical model computer implementation algorithm

An algorithm of computer implementation of the proposed mathematical model is described below.

1. The codes corresponding to the values of constants and parameters necessary for the realization of computer model of MagAmp switch B-H characteristic are entered into the microcontroller's memory registers. They are π, own frequency of the digital generator of sinusoidal signals f; discretization frequency F (it equals to the discretization frequency of the signals within a particular electric circuits computer-aided design (CAD) programme); coefficient that determins the beginning phase *beg* of the waveform of sinusoidal signals digital generator. The user indicates the saturation induction B_s and coercive force H_c values.
2. The output model parameters are calculated with the following equations:
   The step of discretization

$$Teta = 2\pi \frac{f}{F} \quad ; \tag{5}$$

the beginning phase of the waveform

$$Tetab = beg \cdot Teta \; ; \tag{6}$$

coefficient of the digital generator of sinusoidal signals

$$b = 2 \cdot \cos(2\pi \frac{f}{F}) ; \tag{7}$$

the number of points within a half period of the sine waveform

$$k_{\max} = \frac{F}{2f} ; \tag{8}$$

the maximum value of coercive force

$$H_{\max} = H_c + H(k_{\max}) ; \tag{9}$$

the minimum value of coercive force

$$H_{\min} = H(k_1) - 2 \cdot H_c ; \tag{10}$$

3. Initial conditions for the digital generator of sinusoidal signals are set

$$\begin{aligned} G0 &= \sin Tetab \\ G1 &= \sin(Tetab + Teta) \end{aligned} \tag{11}$$

4. The two sequently generated code values (points on the sine waveform) g_{n-1} and g_n are compared
   a. If $g_n > g_{n-1}$ then, taking into account the initial conditions for the digital generator of sinusoidal signals (), a point on the upward part of the sine waveform is digitally generated. This point belongs to a model of a part of B-H characteristic that corresponds to the MagAmp switch transition to conductive state (MagAmp saturation):
   for k=1:n_{max}
   GF(k)=G0;
   GS(k)=G1;
   G=b*G0-G1;
   G1=G0;
   G0=G;
   H(k)=n;
   B(k)=G;
   b. If $g_n < g_{n-1}$ then a point is generated on downward part of the sine waveform which represents a part of B-H characteristic corresponding for MagAmp switch transition from on-state to off-state (from conductive to nonconductive state). Recursive computation is used here:
   for k=1:n_{max}
   GF(k)=G0;
   GS(k)=G1;
   M0=GF(n_{max+1}-n);
   M1=GS(n_{max+1}-n);
   M=b*M0-M1;
   H(k)=n;
   B(k)=M;
   c. When three subsequently generated codes of points on MagAmp switch B-H characteristic are equal $g_n = g_{n-1}$, $g_{n-1} = g_{n-2}$ then they are compared to the code of saturation inductance value B_s.
      i. If $g_n \leq -B_s$ then a code value is generated which corresponds to a point on lower horizontal part of MagAmp B-H characteristic, which represents MaAmp switch off-state (nonconductive state):
      $H_n = H_{min} \ldots H_{min} + 2H_c$
      $B_n = -B_s$;
      ii. If $g_n \geq B_s$ then a code value is generated which corresponds to a point on upper horizontal part of MagAmp B-H characteristic, which represents MaAmp switch on-state (conductive state):
      $H_n = H_{max} \ldots H_{max} - 2H_c$
      $B_n = B_s$.

The block-scheme of the algorithm of high-frequency MagAmp switch B-H characteristic computer model is shown in figure 2.

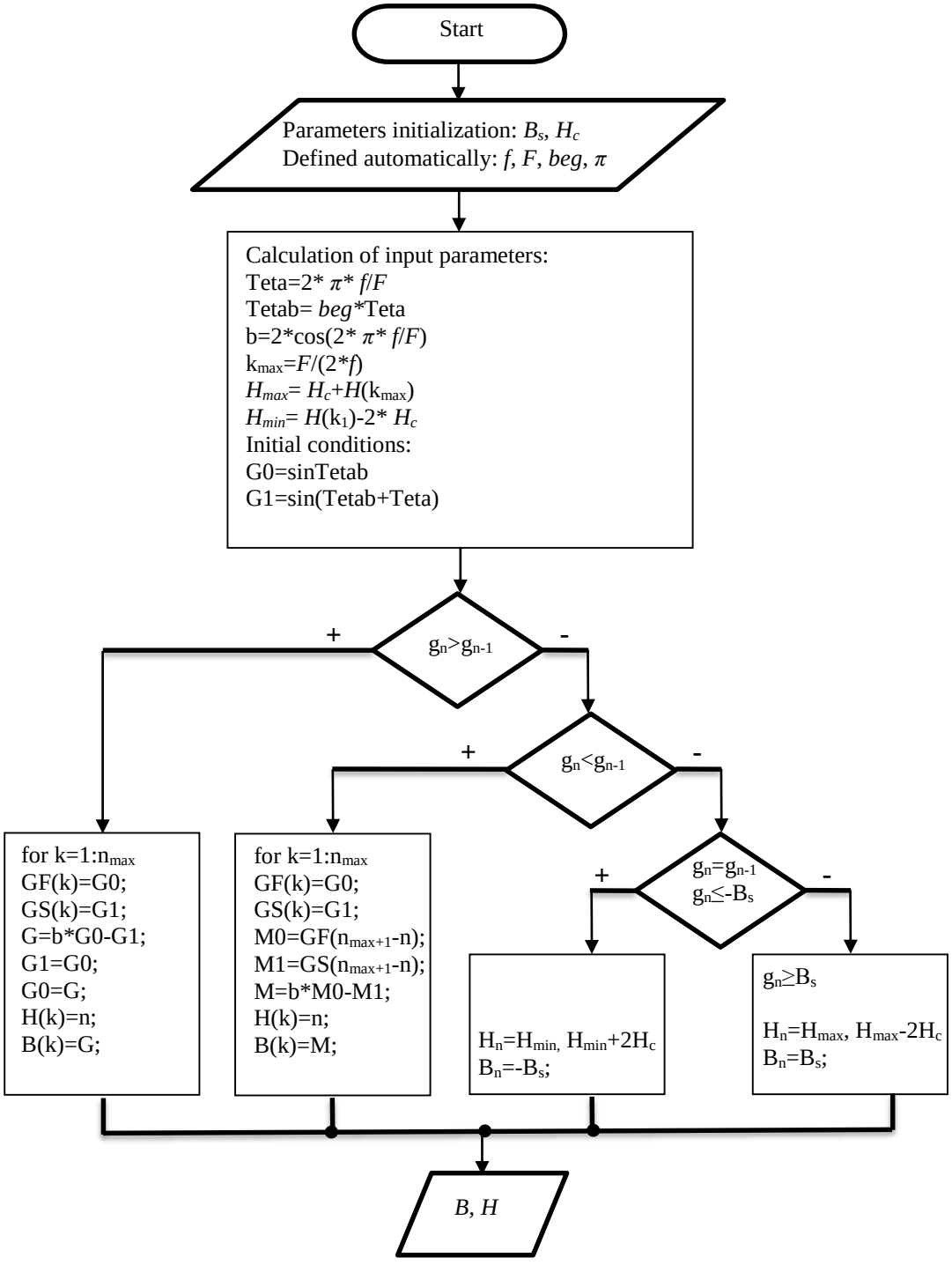

Fig. 2. Block-scheme of the algorithm of high-frequency MagAmp switch B-H characteristic computer model

4. Investigation of modeling capabilities of MagAmp switch B-H characteristic frequency dependence

The results of experimental investigation of MagAmp switch (with parameters: k_r=0,9997, d_{out}=16 мм, d_{in}=7 мм, h=5 мм, N=10) B-H characteristic dependence on the switching frequency are presented on fig.3. Tektronix TDS 1002 oscilloscope with discretization frequency of 60MHz was used.

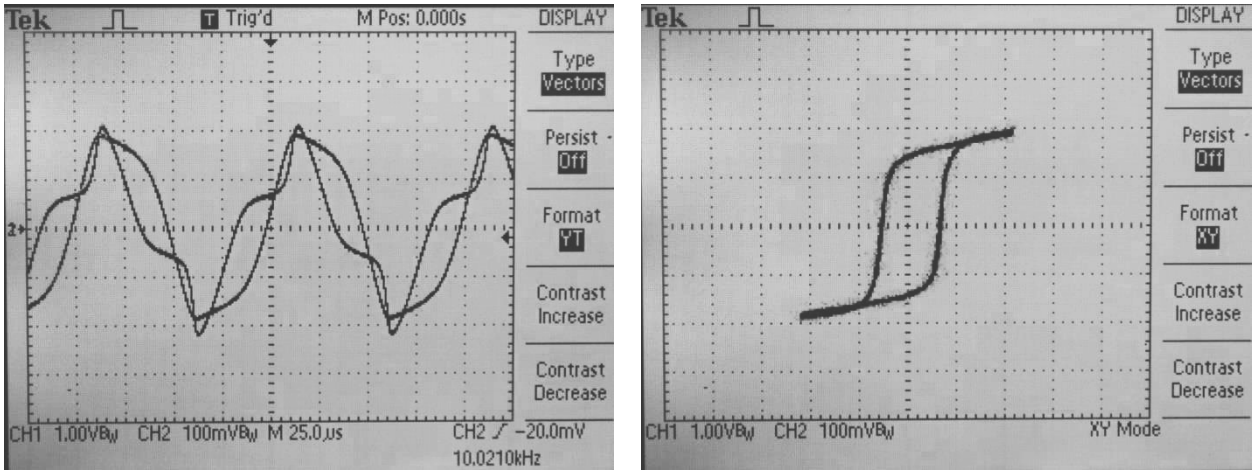

a) MagAmp switch waveforms and B-H characteristic at switching frequency *f*=10kHz

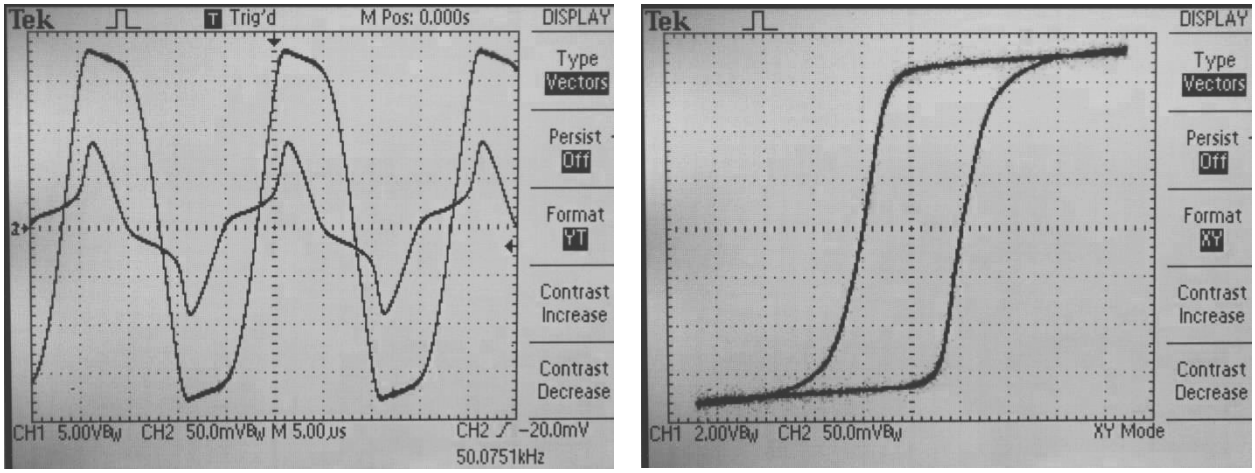

b) MagAmp switch waveforms and B-H characteristic at switching frequency *f*=50kHz

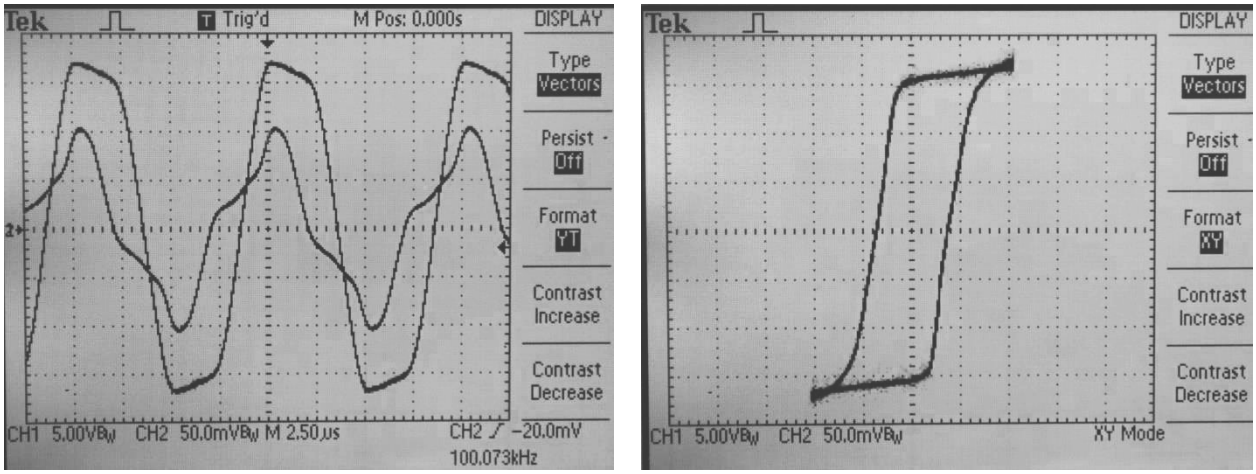

c) MagAmp switch waveforms and B-H characteristic at switching frequency *f*=100kHz

Fig. 3. Dependence of B-H characteristic on the frequency of MagAmp switch with the following parameters: k_r=0,9997, d_{out}=16 мм, d_{in}=7 мм, *h*=5 мм, *N*=10

The results of experimental investigation of MagAmp switch (with parameters: k_r=0,9997, d_{out}=27 мм, d_{in}=18 мм, *h*=12 мм, *N*=10) B-H characteristic dependence on the switching frequency are presented below.

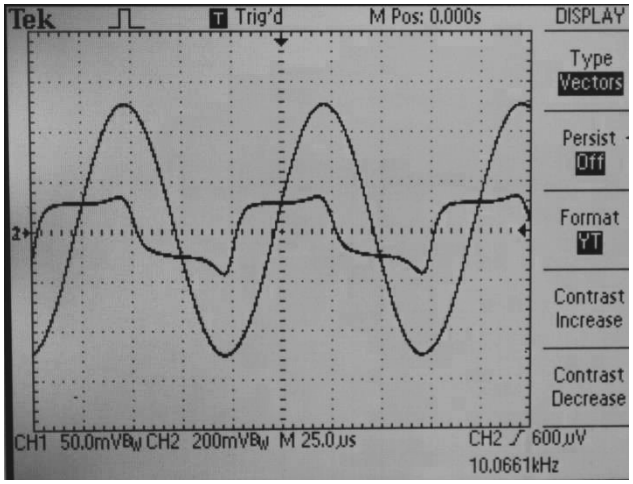

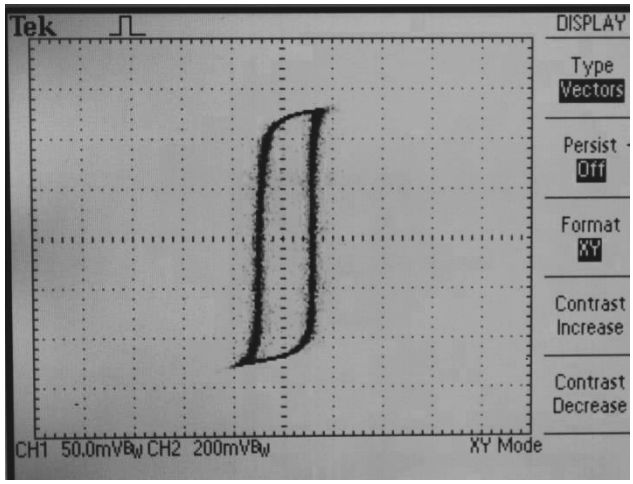

a) MagAmp switch waveforms and B-H characteristic at switching frequency *f*=10kHz

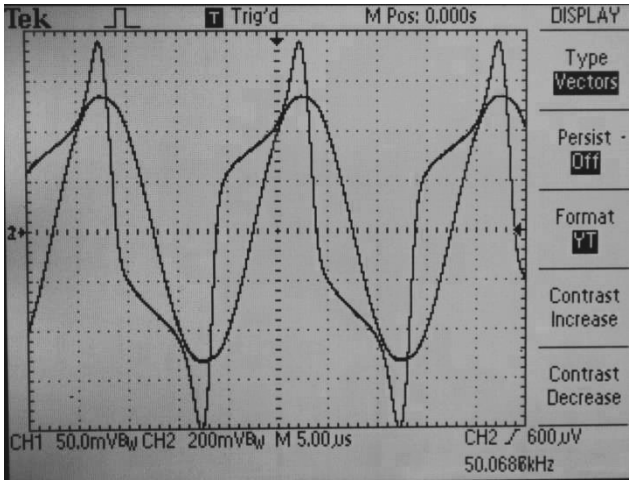

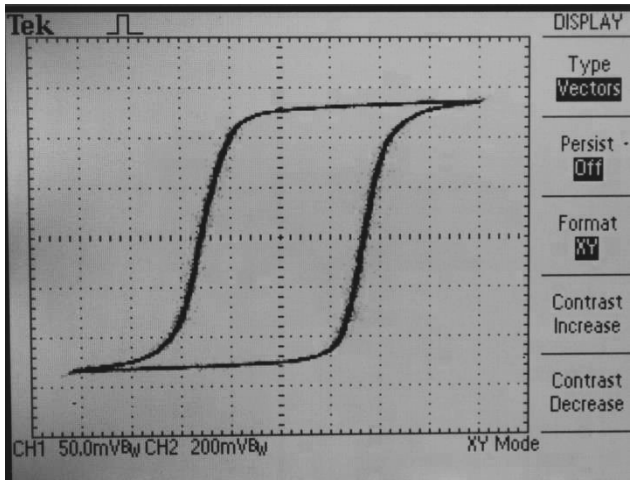

b) MagAmp switch waveforms and B-H characteristic at switching frequency *f*=50kHz

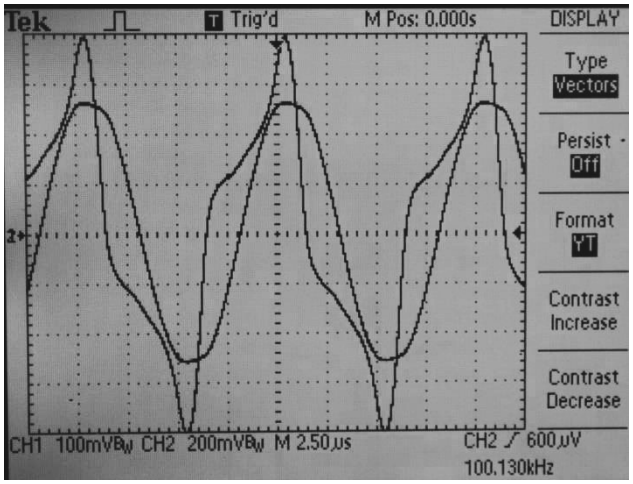

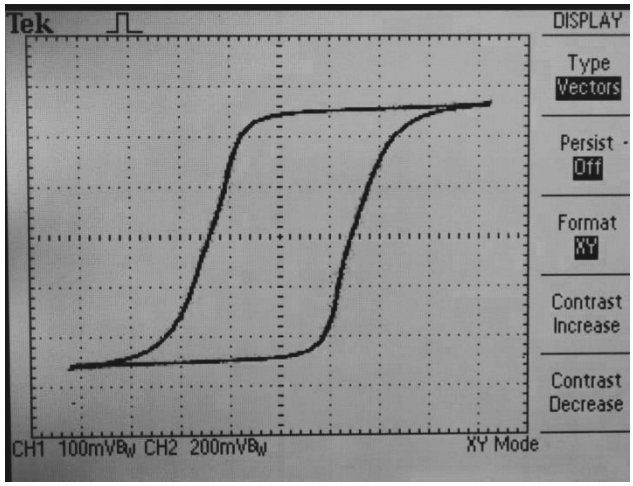

c) MagAmp switch waveforms and B-H characteristic at switching frequency *f*=100kHz

Fig. 4. Dependence of B-H characteristic on the frequency of MagAmp switch with the following parameters: k_r=0,9997, d_{out}=27 мм, d_{in}=18 мм, *h*=12 мм, *N*=10

The experimental results (fig. 3,4) prove that in both cases for the same MagAmp switch B-H characteristic changes depending on the switching frequency: the higher the frequency is, the wider is thehysteresis loop.

Change of the model's input parameters (coercive force, frequency of the generator, discretization frequency, beginning phase of the waveform, and the number of points needed to be generated) provides the regulation of steepness (fig. 5. a)) and width (fig. 5. b)) of the modelled hysteresis loop.

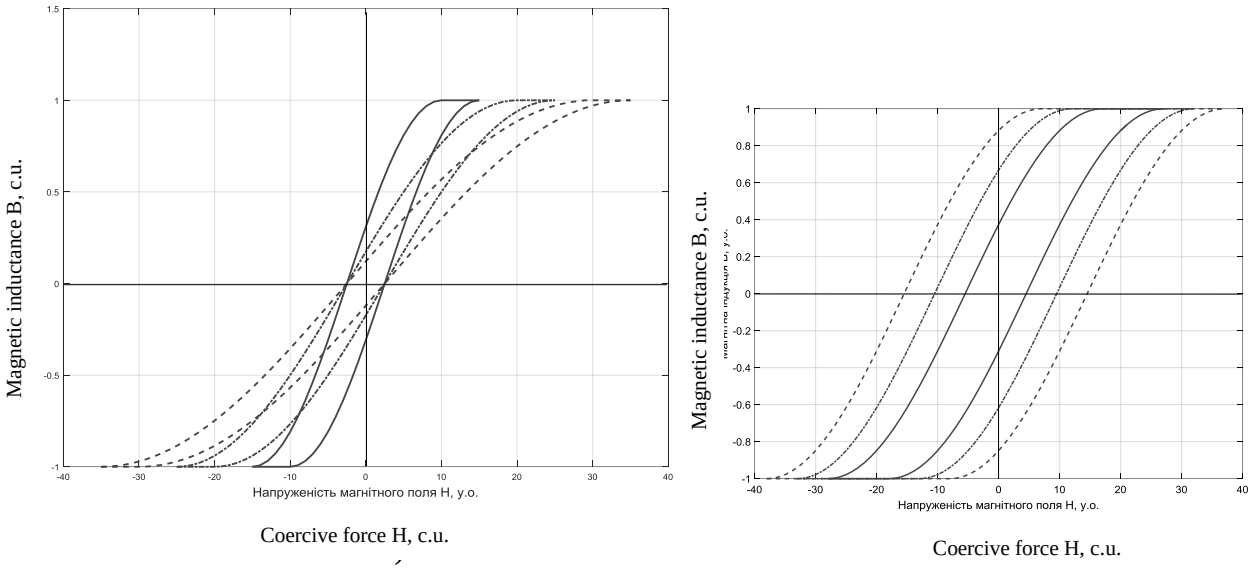

a) **b)**

Fig. 5. Computer realization of the mathematical model of B-H characteristic: a) dependence of the steepness of B-H characteristic model on the change of the ratio of discretization frequency *F* to the own frequency of the generator *f*; b) models of B-H characteristics with different values of coercive force H_c

The *H*, *B* axes values on Fig. 5 are given in conditional units (c. u.). Ratio of the oscilloscope and generator frequencies equals to the number of data points generated during one period (represented along H axes).

The calculated error of B-H characteristic modeling is ≤17,2%, which is smaller than the error of known magnetic hysteresis models, and can be further decreased by taking into account the slope of nearly horizontal parts of the loop (1-2 and 3-4, fig.1).

5.Conclusions

The use of basic digital components for the computer realization of proposed B-H characteristic mathematical model allows its integration in any CAD programme for electric circuits without any additional integrations.

The time complexity of the proposed model of MagAmp switch B-H characteristic is decreased, compared to A. Nicolaide's analytic model of magnetic hysteresis [17,18] which features a somewhat similar structure, however, the number of model's segments was decreased from 6 to 4. Moreover, A.Nicolaide's model is not suitable for power converters design automation, since its LabView integration [18] deals with magnetic fields only.

All input parameters of the proposed model are easy to find in any MagAmp datasheet, which eliminates an existing problem of parameters extraction for known models.

References

1. **Lee, J.; Chen, D. Y.; Jamerson, C.** Magamp postregulators – practical design considerations to allow operation under extreme loading conditions. Proceedings of IEEE APEC. **1988**. P. 368-376.
2. **Austrin, L.; Figueroa-Karlstrom, E.; Engdahl, G.** Evaluation of switching losses in magnetic amplifiers as an alternative to IGBT switching technologies. 4th IET International Conference on Power Electronics, Machines and Drives (PEMD 2008). **2008**. P. 250–254.
3. **Austrin L.** 2007. On Magnetic Amplifiers in Aircraft Applications. Royal Institute of Technology. Sweden. 98 p.
4. **NASA Technical Reports Server (NTRS) 19940009938:** Large space structures and systems in the space station era: A bibliography with indexes (supplement 05). 139 p. Available at: https://archive.org/details/NASA_NTRS_Archive_19940009938/page/n145/mode/2up.
5. **Toshiba**. Saturable cores for mag-amps. Available at: https://pdf.directindustry.com/pdf/toshiba-america-electronics-components/saturable-cores-mag-amps/33679-562725.html#search-en-saturable-cores-mag-amps.
6. **Chen, W.; Hui, S. Y.** A Dimmable Light-Emitting Diode (LED) Driver with Mag-Amp Postregulators for Multistring Applications. IEEE Transactions on Power Electronics. **2011**. Vol. 26, No 6. P. 1714–1722.
7. **Yaskiv, V.; Abramovitz, A.; Smedley, K.; Yaskiv, A.** 2015. MagAmp Regulated Isolated AC-DC Converter with High Power Factor. Special issue of journal COMMUNICATIONS - Scientific Letters of the University of Zilina, ISSN 1335-4205. No. 1A/2015. P. 28-34.
8. **Tatevosian, A. S.; Zaharova, N. V.; Shelkovnikov, S. V**. 2016. Eksperementalnoe issledovanie i raschet magnitnogo polia elektromagnita postoyannogo toka s rasshcheplennymi poliusami i poliusnymi nakonechnikami v

komplekse program ELCUT. Izvestiya Tomskogo politehnicheskogo universiteta. Inzhiniring georesursov, Vol.327, No 2, pp. 133-140. [In Russian]

9. **ANSYS Inc**. Balance of power. ANSYS Advantage, Vol. 8, No 2, 2014, pp. 33-35. Available at: https://www.ansys.com/-/media/ansys/corporate/resourcelibrary/article/balance-of-power-multiphysics-aa-v8-i2.pdf .
10. **Klatt, R.; Krawczyk, F.; Novender, W.-R.; Palm, C.; Weiland T**. MAFIA – A three-dimensional electromagnetic CAD system for magnets, RF structures, and transient wake-field calculations. Proceedings of the **1986** International Linac Conference, Stanford, California, USA. P. 276-278.
11. **Jiles, D. C.; Atherton, D. L**. Theory of Ferromagnetic Hysteresis. J. Magn. And Magn. Mater. **1986**. No 61. P. 48–60.
12. **Chan, J. H.; Vladimirescu, A.; Gao, A., X.; Liebmann, P.; Valainis, J**. Nonlinear Transformer Model for Circuit Simulation. IEEE Transactions on Computer-Aided Design, **1991**, Vol. 10, No 4, pp. 476 – 482.
13. **Yaskiv, A**. Matematychne modeliuvannia protsesiv peremagnichennia magnitomyakyh materialiv z vysokoyu krutyznoyu petli gisterezysu. Mizhnarodnyi naukovo-tehnichnyi zhurnal Vymiriuvalna ta Obchysliuvalna Tehnika v Tehnologichnyh Protsesah, **2015**, No 4 (53), pp. 112-118. [In Ukrainian]
14. **Preisach, F**. Uber die magnetische Nachwirkung. Zeitschrift fur Physik. **1935**. No 94. P. 861–890.
15. **Adly, A. A.; Abd-El-Hafiz, S. K.** Efficient modeling of vector hysteresis using a novel Hopfield neural network implementation of Stoner–Wohlfarth-like operators. Journal of Advanced Research. **2013**. No 4. P. 403–409.
16. **Konieczny, J., Dobrzañski, L. A., Tomiczek, B., Trzaska, J**. Application of the artificial neural networks for prediction of magnetic saturation of metallic amorphous alloys. Archives of Materials Science and Engineering. **2008.** Vol. 30, No 2. P. 105–108.
17. **Nicolaide, A**. An Approach to the Mathematical Modeling of the Hysteresis Curves of Magnetic Materials: the Minor Curves**. 2007**. P. 301-310.
18. **Motoasca, S.; Scutaru, G**. Hysteresis modeling of soft magnetic materials using LabView Programs. Advances in Electrical and Computer Engineering. **2010**. Vol 10, No 2. P.94-97.
19. **Edry, D., Ben-Yaakov, S**. A SPICE Compatible Model of Magamp Post. Regulators. *IEEE Applied Power Electronics Conf., APEC'92*. **1992**. P. 793 – 800.
20. **Yaskiv, A., Yavorskyy, B.** Integration of Magnetic Amplifier Switch Model into Computer Aided Design for Power Converters. Scientific journal of TNTU. **2019**. No 2 (94). P. 123-133.